Lasers in Surgery and Medicine 30:141–148 (2002)
DOI 10.1002/lsm.10015

Clinical Testing of a Photoacoustic Probe for Port Wine Stain Depth Determination

John A. Viator, PhD,[1]* Gigi Au,[1,2] Guenther Paltauf, PhD,[3] Steven L. Jacques, PhD,[4] Scott A. Prahl, PhD,[4] Hongwu Ren, PhD,[1] Zhongping Chen, PhD,[1] and J. Stuart Nelson, MD, PhD[1]
[1]*Beckman Laser Institute and Medical Clinic, Irvine, California 92612*
[2]*Harvey Mudd College, Claremont, California 91711*
[3]*Karl-Franzens-Universität Graz, Graz, Austria*
[4]*Oregon Health and Science University, Portland, Oregon 97291*

Background and Objective: Successful laser treatment of port wine stain (PWS) birthmarks requires knowledge of lesion geometry. Laser parameters, such as pulse duration, wavelength, and radiant exposure, and other treatment parameters, such as cryogen spurt duration, need to be optimized according to epidermal melanin content and lesion depth. We designed, constructed, and clinically tested a photoacoustic probe for PWS depth determination.
Study Design/Materials and Methods: Energy from a frequency-doubled, Nd:YAG laser ($\lambda = 532$ nm, $\tau_p = 4$ nanoseconds) was coupled into two 1,500 μm optical fibers fitted into an acrylic handpiece containing a piezoelectric acoustic detector. Laser light induced photoacoustic waves in tissue phantoms and a patient's PWS. The photoacoustic propagation time was used to calculate the depth of the embedded absorbers and PWS lesion.
Results: Calculated chromophore depths in tissue phantoms were within 10% of the actual depths of the phantoms. PWS depths were calculated as the sum of the epidermal thickness, determined by optical coherence tomography (OCT), and the epidermal-to-PWS thickness, determined photoacoustically. PWS depths were all in the range of 310–570 μm. The experimentally determined PWS depths were within 20% of those measured by optical Doppler tomography (ODT).
Conclusions: PWS lesion depth can be determined by a photoacoustic method that utilizes acoustic propagation time. Lasers Surg. Med. 30:141–148, 2002.

Key words: optoacoustic; PVDF; acoustic transducer; Q-switched; acrylamide; optical fiber; skin

INTRODUCTION

Photoacoustics in biomedical optics may be described as a laser induced ultrasound. However, while conventional ultrasound detects interfaces of different acoustic impedances, laser light in photoacoustics is transduced into acoustic energy so that the region of interest becomes an active source. If the laser wavelength is chosen so that the intended target absorbs well, high acoustic contrast will result, making it possible to locate the target. Also, due to the transduction mechanism, the resultant acoustic wave can be analyzed for the target's optical properties.

Photoacoustic measurements have been used to detect subsurface chromophores in tissue and tissue-like media. Esenaliev et al. [1] localized small, optically absorbing spheres in tissue and tissue-like media. Viator et al. [2] determined optical absorption coefficients as a function of depth in tissue phantoms and a stained elastin biomaterial. Viator et al. [3] determined the thickness of a turbid gel over an absorbing layer as a model of necrotic tissue over normally perfused tissue after photodynamic therapy. The latter application can be adapted to the problem of port wine stain (PWS) depth determination, which would aid in the treatment of these lesions.

Successful laser treatment of PWS is intimately related to skin structure with emphasis on the optical and thermal properties of the epidermal, dermal, and PWS layers [4–6]. The goal of PWS treatment is photothermal coagulation of the ectatic blood vessels by laser irradiation without causing epidermal damage. Cryogen spray cooling (CSC) allows for selective cooling of the epidermal melanin layer while maintaining the normal physiological temperature of the PWS blood vessels. Spatially selective cooling of the epidermis enables the physician to increase the laser fluence, since the energy required to reach threshold for epidermal damage is greater. Laser fluence and thermal diffusion from the PWS to the cooled epidermis both depend on PWS depth. Therefore, optimal treatment of PWS requires knowledge of lesion depth, which motivates use of the photoacoustic probe described in this article. Because the speed of sound in tissue is known [7], the acoustic propagation time from the PWS to the skin surface can be correlated with lesion depth. This depth obtained

Contract grant sponsor: National Institutes of Health; Contract grant numbers: AR43419, HL-64218, RR-01192, GM62177; Contract grant sponsor: The National Science Foundation; Contract grant number: BES-0086924.
Contract grant sponsor: U.S. Air Force of Scientific Research F49620–00–1–0371.
*Correspondence to: John A. Viator, PhD, Beckman Laser Institute and Medical Clinic, 1002 Health Sciences Road East, Irvine, CA 92612. E-mail: javiator@laser.bli.uci.edu
Accepted 1 October 2001

from photoacoustic measurements can be used by the clinician to optimize laser and CSC parameters.

In this article, we describe the design, construction, and clinical testing of a probe to determine the depth of subsurface chromophores from the acoustic propagation time. The probe was designed to measure PWS depth in human skin in a non-invasive manner.

MATERIALS AND METHODS

Photoacoustic Probe Construction

The photoacoustic probe consisted of two 1,500 μm optical fibers inserted at a 10° angle into a cylindrical acrylic handpiece (Fig. 1). A rigid copper coaxial cable was inserted into the handpiece and terminated with a polyvinylidene fluoride (PVDF) film that served as the active area of the acoustic detector. The 1.1 mm diameter coaxial cable (UT-43-10, Micro-Coax, Pottstown, PA), with an impedance of 10Ω, was used as the electronic transmission line for a piezoelectric film sensor. The sensor was a bi-directional, 25 μm thick PVDF film (K-tech, Albuquerque, NM), aluminized on one side. The film was cut into a 1.2 mm circle and fitted onto the cleaved and polished face of the coaxial cable (Fig. 2). The ends of the fibers and coaxial cable were oriented within a chamber at the distal end of the handpiece. The chamber had inlet and outlet ports so that it could be filled with water, to ensure good acoustic coupling to the phantoms or human skin. Setscrews were used to steer the fibers so that the acoustic sensor was directly over the laser irradiated spot. The non-aluminized bottom layer of the film was epoxied to the 700 μm diameter center conductor of the cable, while the aluminized top layer was connected to the outer conductor. Conducting paste (Conducting Pen, CircuitWorks, Inc., Garland, TX) was used to connect the film to the outer conductor of the coaxial cable. Thus, the aluminized top layer and the circular face of the center conductor served as the two electrodes sensing the electric field created by PVDF deformation due to the acoustic wave. The probe was utilized by delivering laser energy through the fibers that induced photoacoustic waves in the optically absorbing medium, which were subsequently sensed by the transducer. In order to prevent electrical noise of the laser from interfering with acoustic wave detection, the trans-

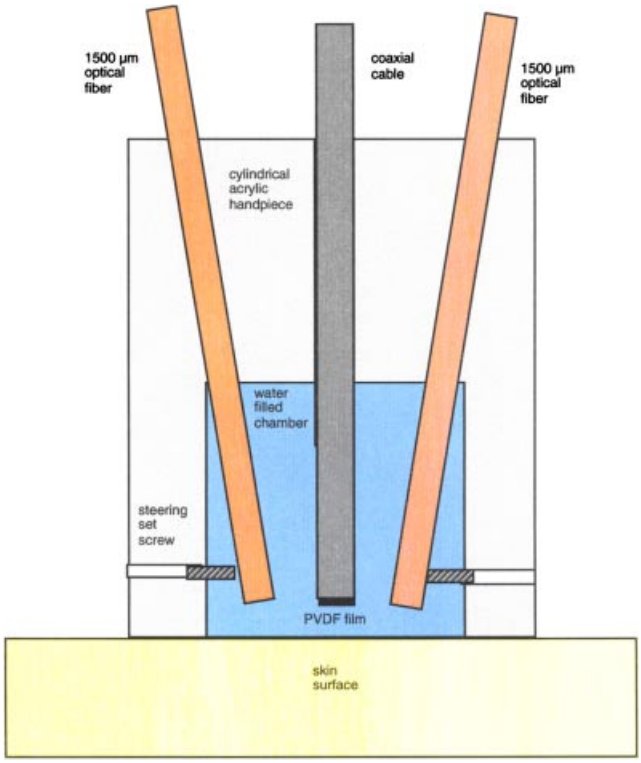

Fig. 1. The photoacoustic probe consisted of a piezoelectric film at the tip of a rigid coaxial cable inserted into a cylindrical acrylic housing. The 1,500 μm optical fibers were inserted into the acrylic cylinder to irradiate an embedded absorber, inducing a photoacoustic wave. The PVDF film was placed at the tip of the coaxial cable to create an acoustic sensor.

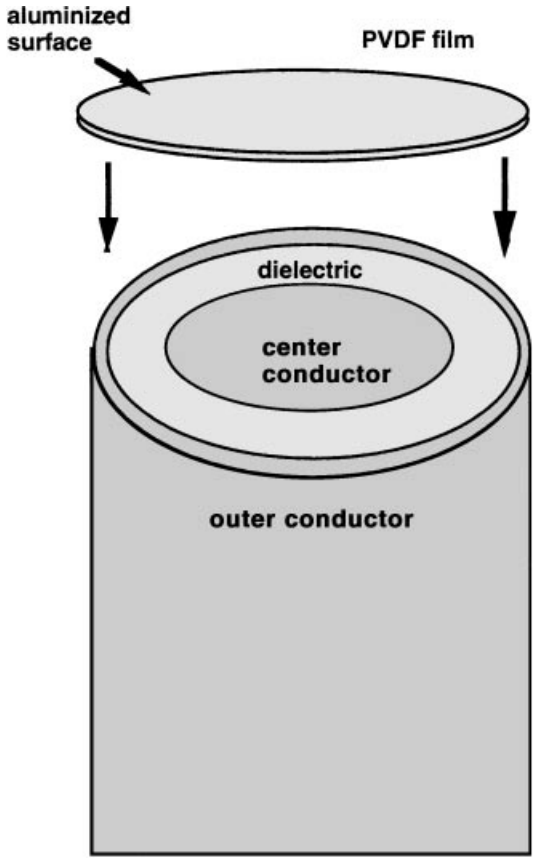

Fig. 2. The acoustic transducer was made by attaching a circular PVDF film to a semi-rigid coaxial cable. The center conductor of the coaxial cable served as one capacitive plate of the piezoelectric detector, while a thin aluminum layer on the top side of the PVDF, which was electrically connected to the outer conductor, served as the other capacitive plate. The outer conductor was connected to the aluminum layer by a conducting paste.

ducer active area was recessed approximately 3 mm from the bottom of the acrylic handpiece to create an acoustic delay line. In tissue or water, where the speed of sound is approximately 1.5 mm/μsec, the delay was approximately 2.0 microseconds. The exact delay was determined using the procedure described below.

Experimental Apparatus

The experimental apparatus shown in Figure 3 consisted of a frequency-doubled Nd:YAG laser (Quantel Brilliant, Big Sky Laser, Bozeman, MT) operating at 532 nm, with a pulse duration of 4 nanoseconds. The beam was split and focused by plano-convex lenses into two 1,500 μm fibers. To avoid optical breakdown of the fibers, a neutral density filter with a 0.9 optical density was used to attenuate the laser energy. The beam energy was 180 mJ with a pulse repetition rate of 10 Hz. Laser energy at the output of each fiber was 11 mJ. The laser spot area was determined by irradiating thermal paper. The radiant exposure was then calculated to be 0.08 J/cm^2. The sensing element, fibers, coaxial cable, and acrylic handpiece constituted the photoacoustic probe that was put in direct contact with tissue phantoms and PWS skin of a volunteer subject. The targets were irradiated and the resultant photoacoustic signals sensed by the PVDF film. The acoustic signal was transduced by the PVDF into an electrical signal, which was sent to an oscilloscope (TDS 3054, Tektronix, Wilsonville, OR) with a bandwidth of 500 MHz and an input impedance of 1 MΩ. The high input impedance resulted in a displayed waveform corresponding to acoustic pressure. The waveform was analyzed for acoustic propagation time to determine the depth of the absorbing layer.

OCT/ODT Measurements

Photoacoustic measurements of the PWS were compared to those at the same sites using ODT. OCT measurements were taken to determine the epidermal thickness of the test sites [8,9]. This thickness was added to the photoacoustically measured epidermal-to-PWS distance to determine lesion depth.

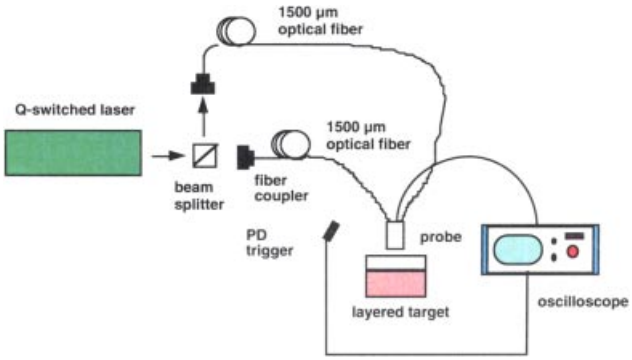

Fig. 3. Experimental apparatus. A Q-switched Nd:YAG laser operating at 532 nm delivered 4 nanoseconds laser pulses into two 1,500 μm fibers directed to a layered absorbing target. The resultant photoacoustic wave was detected by a PVDF transducer and sent to an oscilloscope triggered from a fast photodiode.

Tissue Phantoms

Acrylamide gel phantoms were used to simulate multilayered composite human skin with a non-absorbing layer resting on an absorbing layer. These gels were used to calibrate the acoustic delay in the probe. The 20% acrylamide was made by adding 9.7 g of acrylamide and 0.3 g of bis-acrylamide (Sigma Chemical, St. Louis, MO) to 50 ml of deionized water. Direct Red 81 (Sigma Chemical) was used to create optical absorption at 532 nm. The optical absorption of the dye was determined with a spectrophotometer (8452A Diode Array Spectrometer, Hewlett Packard, Waldbronn, FRG). Ammonium persulfate and tetra-methylethylenediamine (TEMED) (Sigma Chemical) were used to initiate polymerization of the solution into a gel.

Skin phantoms were made by creating acrylamide layers of different thicknesses, as previously described [2,10]. Acrylamide solutions were injected between glass slides with plastic feeler gauge stock (McMaster-Carr, Los Angeles, CA) used as spacers. Thicknesses of the feeler gauge stock and gels were verified using a micrometer with 1 μm resolution and 1 μm accuracy (Mitutoyo micrometer, McMaster-Carr). Layered gels were made with a non-absorbing layer set on an absorbing substrate with an absorption coefficient of 118 cm^{-1} at 532 nm. The clear layers had thicknesses of 100, 300, 500, 700, and 900 μm. These depths were chosen to achieve precise measurements of the acoustic delays.

Transducer Calibration

The detector was calibrated by inducing photoacoustic waves in solutions where the absorption coefficient was known. The PVDF sensor detected the waves in a transmission setup which was chosen to maximize signal strength and reproducibility of measurements. The free beam of the laser was used, providing a large spot that minimized diffraction and delivered more energy. The detectors were immersed in absorbing solutions and centered directly above the laser spot. Several detectors were tested in this manner and the most sensitive was chosen for use with the photoacoustic probe. The laser spot diameter was 4.6 mm. The radiant exposure was 0.084 J/cm^2 as calculated by measuring total energy with a detector, (Molectron, Beaverton, OR) and dividing by the spot size. The absorption coefficients of the solutions were 51, 103, 148, 197, and 239 cm^{-1} at 532 nm. The solution thickness of 3 mm was chosen so that no laser irradiation would reach and damage the acoustic sensor.

The equation

$$p(0) = \frac{1}{2}\Gamma H_0 \mu_a \tag{1}$$

was used to predict the photoacoustic pressure (J/cm^3). Viscoelastic attenuation was neglected in this analysis. Γ is the Grüneisen coefficient, which models the fraction of optical energy converted to acoustic energy. In this

analysis, $\Gamma = 0.12$ was used [11,12]. H_0 is the radiant exposure (J/cm^2), and μ_a is the absorption coefficient of the solution in cm^{-1}. Finally, the conversion 10 bar $= 1$ J/cm^3 was used to determine a calibration factor of mV/bar for the acoustic detector by dividing the amplitude of the acoustic waveform by the calculated pressure.

In Vitro Testing

The propagation time of the photoacoustic waves corresponded to the thicknesses of the clear layer in addition to the distance that the piezoelectric film was inset into the probe. Using the acoustic propagation times from the various thickness phantoms, the intrinsic delay of the probe was calculated. This delay time was subtracted from the total propagation time to determine the depth of the absorbing layers. All recorded waveforms were averaged over 16 signals. The peak amplitude was chosen to delineate the layer depth, as the highest pressure amplitude corresponded with the surface of the dyed gel, since the laser fluence was highest there. Signal to noise ratio (SNR) was determined by dividing the peak amplitude by the noise. The noise level was calculated by the average difference in amplitude from the positive to negative peaks in the oscilloscope trace before any acoustic event was detected.

Clinical Testing

Clinical testing was conducted according to the procedures used in testing gel phantoms. Unlike the flat gel samples, skin at the test sites was not coplanar with the bottom of the acrylic handpiece. Bulging of the skin into the water filled chamber decreased the acoustic propagation delay time, making a simple depth measurement impossible. However, the difference in propagation time of the epidermal photoacoustic signal and the PWS signal provided an indication of the distance between the epidermal layer and the lesion. Assuming that the peak epidermal signal came primarily from the basal layer, where melanin concentration is highest, the sum of the epidermal thickness and photoacoustically determined epidermal-to-PWS distance should specify PWS depth. For these measurements, OCT was used to determine the epidermal thickness.

The human subject had a PWS on his left upper extremity. Specifically, the probe was placed over his dorsal hand, dorsal ring finger, palm, and palmar ring finger. The probe was placed over these four sites with 16 measurements taken at each site. ODT measurements were recorded at each region, as close as possible to the photoacoustically measured sites.

RESULTS

Acoustic Transducer Calibration

The transducer was calibrated by inducing photoacoustic waves in five dye solutions with known absorption coefficients. The average sensitivity was 1.31 mV/bar.

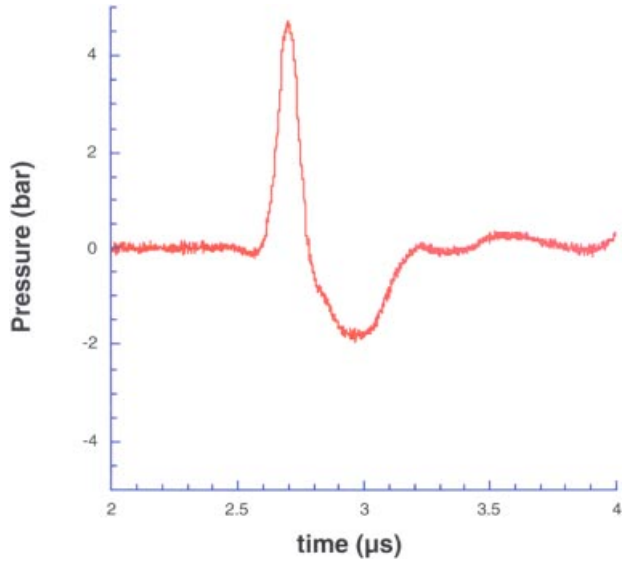

Fig. 4. Typical acoustic wave from the acrylamide phantoms. Clear layer thickness was 500 μm.

In Vitro Testing

The acoustic waveform from an acrylamide phantom with a 500 μm clear layer is shown in Figure 4. The SNR was 80. The acoustic propagation time of the peak was used to determine the clear layer thickness.

The acoustic propagation times for the clear layers are shown in Figure 5. The intrinsic delay of the photoacoustic probe was 2.38 microseconds, as determined by the intercept of the linear fit to the propagation time data with the vertical axis.

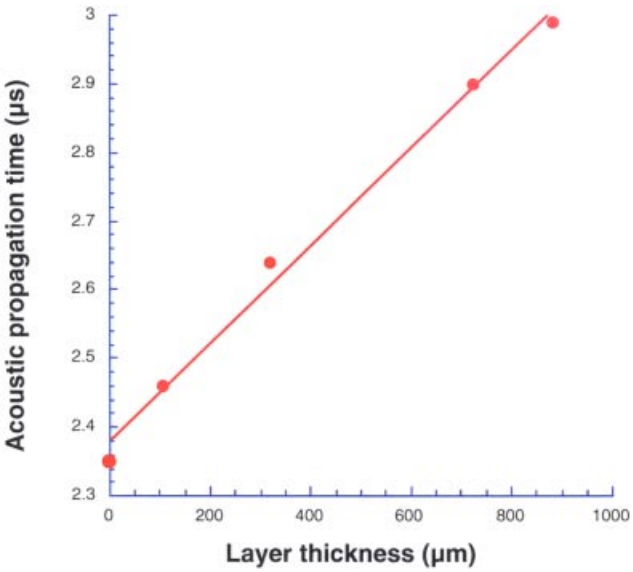

Fig. 5. Acoustic propagation time as a function of depth in the non-turbid gels. The propagation time is the sum of the travel time through the clear layer and the travel time to reach the acoustic inset into the probe. This intrinsic acoustic delay was equal to the intercept of the linear fit on the vertical axis.

Clinical Testing

The photoacoustic signals and OCT and ODT images for the dorsal hand, dorsal ring finger, palm, and palmar ring finger PWS are shown in Figures 6–9, respectively. The SNRs were 10, 16, 22, and 12, respectively.

Averaged PWS depths for the test sites are shown in Table 1. OCT measurements of epidermal thicknesses were added to the photoacoustically derived distances between the epidermal basal layer and the PWS lesion to give a photoacoustically determined PWS depths. The ODT and photoacoustic depths agree to within 20%.

DISCUSSION

The probe was successfully calibrated for acoustic delay and demonstrated the ability to measure the thickness of acrylamide phantoms from 100–900 μm. The probe was also tested on PWS skin with successful acoustic wave detection and subsequent analysis leading to lesion depth determination. While the probe performed successfully, some limitations of the device were noted.

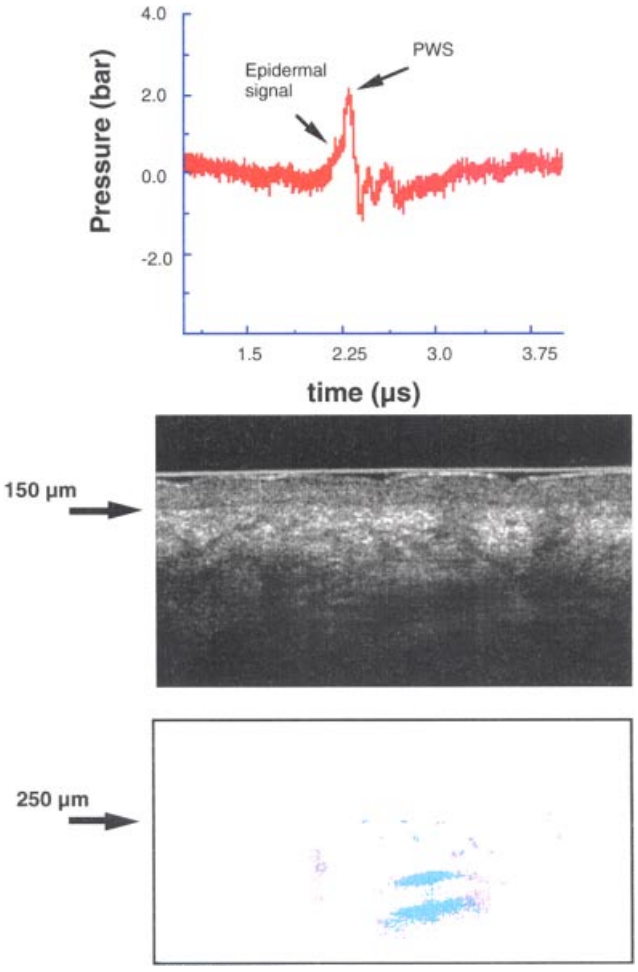

Fig. 6. Measurements on the dorsal hand. The photoacoustic signal shows a small epidermal component nearly overlapping with the PWS signal (top). OCT shows a shallow epidermis (middle). ODT indicates a shallow PWS (bottom).

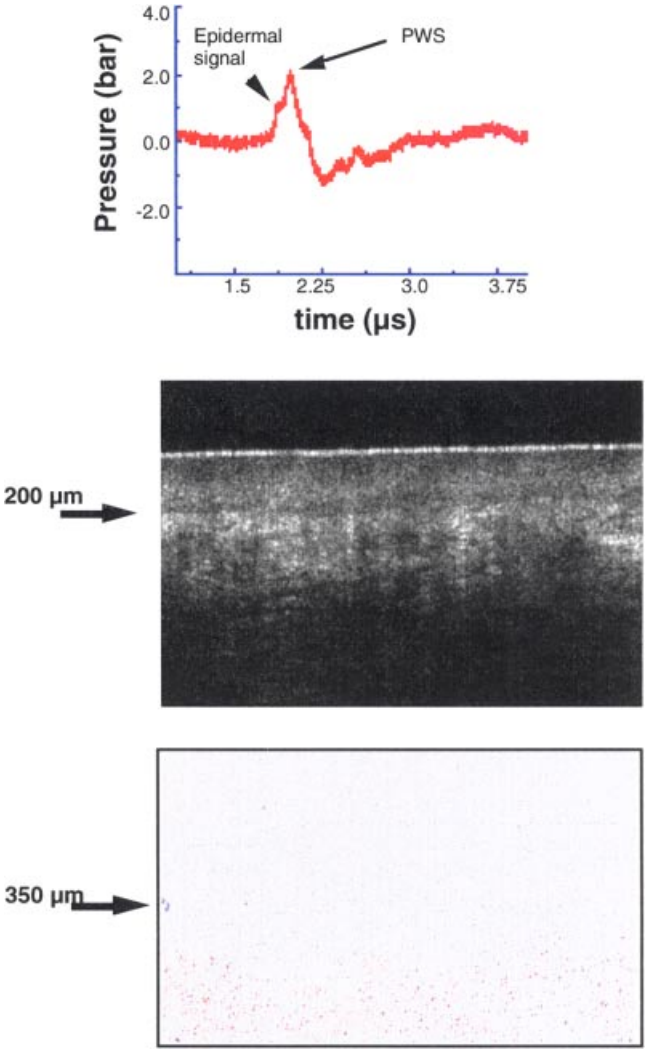

Fig. 7. Measurements on the dorsal ring finger. The epidermal component of the photoacoustic wave significantly overlaps the PWS (top). OCT indicates a slightly thicker epidermis than that of the dorsal hand (middle). ODT shows a small vessel at a depth of 350 μm (bottom).

Phantom Measurements

Depth determined from the acoustic propagation time assumed that the laser spot was incident and the acoustic wave was generated directly below the sensor. With a slight misalignment of the optical fibers, the acoustic propagation time would be increased by $\cos\theta$ where θ is the angle off of the normal vector from the surface. Thus, misalignment of 10° would increase the calculated depth by 10%. The steering set screws, described earlier, were incorporated to ensure proper alignment of the fibers and transducer. When initially testing the probe, the fibers were steered so that the acoustic signal propagation time

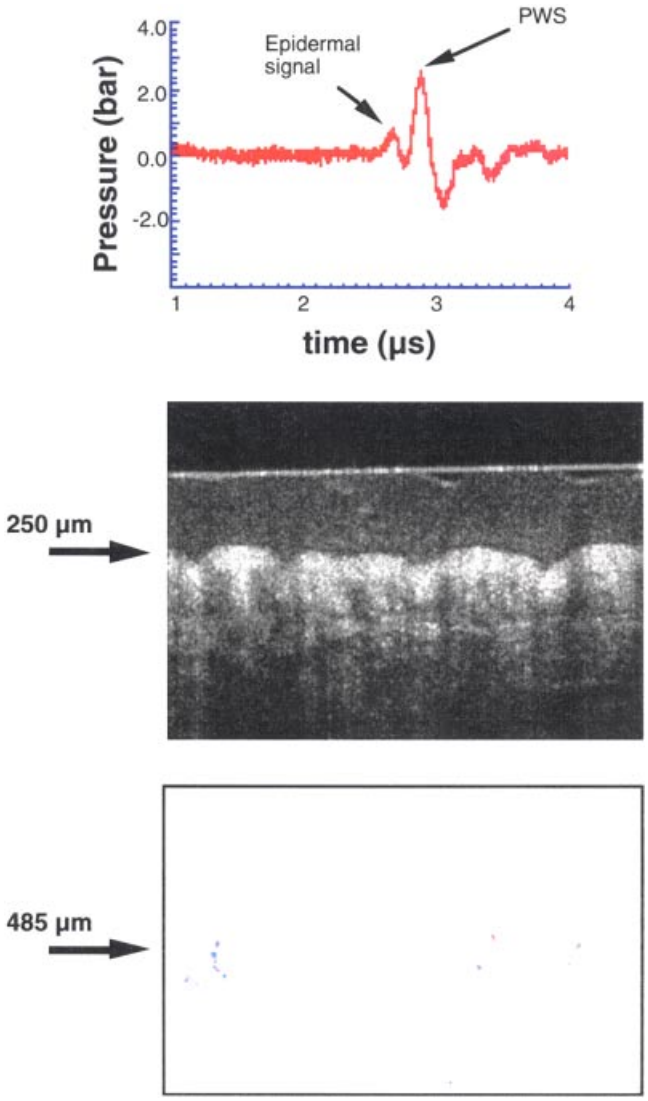

Fig. 8. In the palm, the PWS is much deeper, as indicated by the relatively large separation between the epidermal signal and PWS component (top). OCT shows a thick epidermis (middle). ODT also indicates a much deeper PWS than the two previous measurements from the dorsal hand and ring finger (bottom).

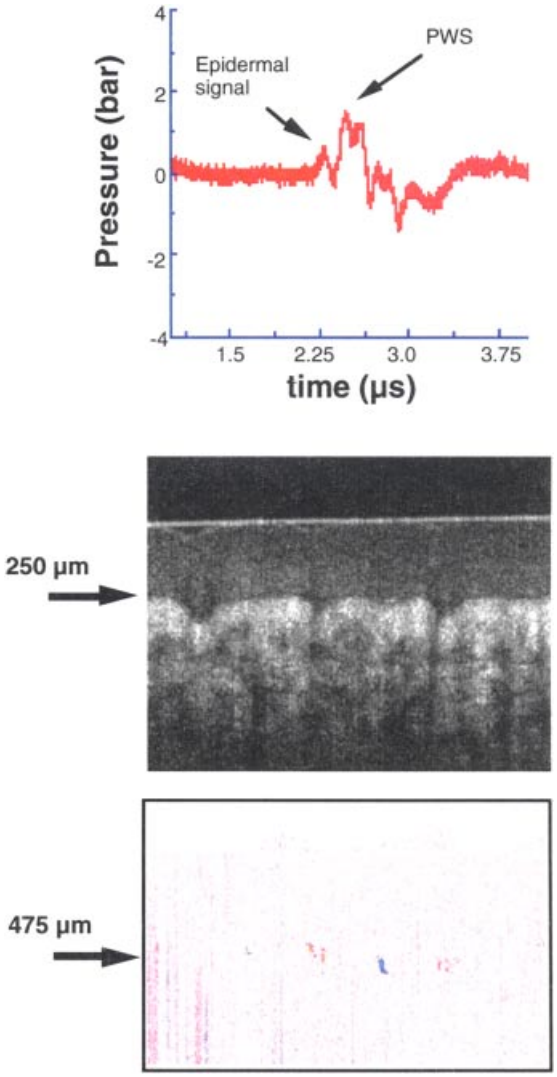

Fig. 9. The palmar ring finger shows the PWS and epidermal signals as distinct, due to the depth of the PWS (top). OCT indicates a thick epidermis (middle). ODT shows PWS at 475 μm (bottom).

TABLE 1. Averaged Depths of Port Wine Stain (PWS) Lesion Sites for the Photoacoustic Methods (PA) Compared to Optical Doppler Tomography (ODT)

Site	Epidermal depth (OCT)	Epidermal-PWS depth (PA)	PWS depth (OCT + PA)	PWS depth (ODT)
Dorsal hand	150	160	310	250
Dorsal ring finger	200	160	360	350
Palm	250	320	570	485
Palmar ring finger	250	250	500	475

The sum of the epidermal thickness from OCT and the epidermal-to-PWS thickness from the photoacoustic probe is indicated as the photoacoustically determined PWS depth.

was minimized, ensuring that the laser spot was incident directly below the acoustic sensor.

Clinical Implementation

The acoustic delays determined from the phantoms was useful only for measurements where the sample surface was coplanar with the bottom of the acrylic handpiece. For skin measurements, some bulging of the skin into the water filled chamber resulted in epidermal signals before the intrinsic delay time of 2.38 microseconds. A glass plate attached to the bottom of the acrylic handpiece would ensure that the skin surface was not bulging into the chamber, but introduces an acoustic interface causing some reflection of acoustic energy away from the detector. Even without a glass plate, the distance from the epidermal basal layer, indicated by the first acoustic peak, and the PWS signal provided the necessary information to determine the distance between the two layers. This distance added to an assumed or measured epidermal thickness determined the actual PWS depth. For CSC, the important information is the difference in depth between the PWS and epidermal melanin layer, since these are the two absorbing structures of interest to the clinician.

The probe was tested on a PWS patient with a low epidermal melanin concentration. Even so, the epidermal melanin signal was useful in determining the distance to the PWS. However, for patients with a high epidermal melanin concentration, laser irradiation would be attenuated to a greater extent, resulting in a weaker PWS signal. Assuming a melanin volume fraction of 2% for a skin type I–II patient [13], an epidermal melanin layer thickness of 50 μm, and melanin absorption coefficient of 400 cm^{-1}, the optical attenuation by the melanin layer is approximately 4%. For a skin type III–V patient with a melanin concentration of 30%, the optical attenuation by the melanin layer is approximately 50%, or a factor of 12 greater. Thus the PWS signal may be obscured for patients with darker skin types, making depth determination impossible. However, a tunable laser, such as an Nd:YAG with an optical parametric oscillator, would allow the clinician to choose the optimal laser wavelength that minimizes melanin absorption while still maintaining high blood absorption. A laser wavelength of 580 nm would maximize hemoglobin absorption, while lowering the melanin absorption by a factor of two [14].

Improvements in Photoacoustic Detection

There are several shortcomings in the current design of the photoacoustic probe. While PVDF is a sensitive piezoelectric element, the small size of the active area may decrease sensitivity. Additionally, a 1,500 μm fiber cannot deliver much more than 11 mJ of laser energy at 532 nm with a pulse duration of 4 nanoseconds without reaching the optical breakdown of the silica fiber face [15]. A possible improvement would be an all optical detection scheme similar to that introduced by Paltauf et al. [12]. Such a system would allow a small active area, created by a focused HeNe probe beam, while allowing delivery of laser energy by a free beam, without having to couple light through an optical fiber. Although such a detector is not as sensitive as PVDF, the increased laser energy would counteract the loss in sensitivity. If the radiant exposure is increased, nonlinear effects may be introduced, which would make depth localization more difficult. A higher radiant exposure would also affect the temperature dependent value of the Grüneisen coefficient, altering the acoustic amplitude, although this would not necessarily affect the propagation time measurement.

Whether utilizing the PVDF sensor or the optical method discussed above, adding a high speed amplifier would increase the acoustic signal and allow a reduction in the radiant exposure and patient discomfort. Even if amplification distorted the signal, the time information would be preserved, which is the primary concern when performing depth measurements.

Depth Profiling

The current probe used a laser wavelength of 532 nm. The absorption depth of whole blood at this wavelength is approximately 50 μm [16], which may be less than the thickness of a single PWS blood vessel, and certainly less than that of a PWS layer [16–18]. Changing the laser wavelength to 600 nm would increase the absorption depth by a factor of fifteen, thus making PWS depth profiling possible, using the tunable system described above. If the increased absorption depth allows full penetration of laser light through the PWS, the resultant photoacoustic wave may indicate the full lesion profile, similar to the layered gel model described by viator et al. [2]. A scan of different wavelengths may provide a range of PWS depth information, enabling the method to produce a photoacoustic profile.

As a preliminary example, a 1 mm thick acrylamide gel with an absorption coefficient of 10 cm^{-1} was irradiated with the probe and the resulting acoustic wave is shown in Figure 10. This signal represented irradiation of a PWS lesion at approximately 600 nm. This signal is much weaker than other phantom measurements, because the absorption coefficient is 90% less than the value of the layers used in the experiments described above. The positive spike at 3.2 microseconds is from the black substrate that the gel rested on. The region between 3.1 and 3.2 microseconds represents a thin, turbid layer between the substrate and gel sample. The waveform from 2.4 to 3.1 microseconds represents a depth profile of the gel. Using the speed of sound of 1.5 mm/μsec, the profile represents a thickness of about 1 mm. Techniques used to increase SNR may allow a plane wave analysis, resulting in an absorption coefficient as a function of depth.

Photoacoustics and OCT/ODT

Although ODT can detect vessels 500 μm below the skin surface, the inherent scattering of tissue makes PWS detection more difficult with increasing depth. The photoacoustic signals in this study had a high SNR, indicating that PWS depth determination could be feasible for lesions

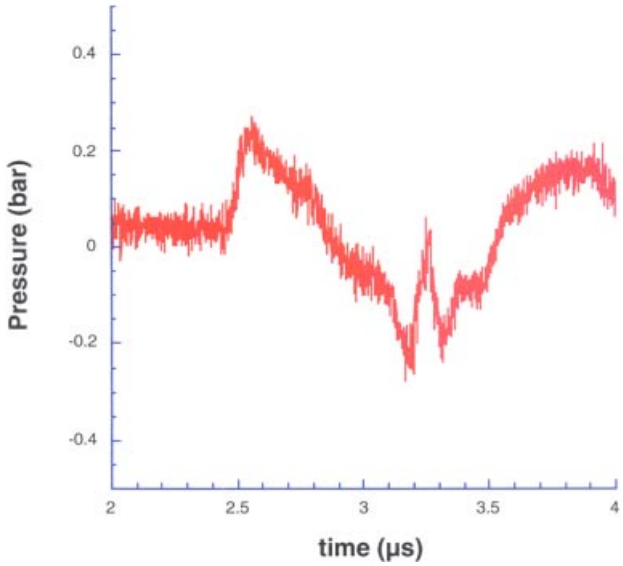

Fig. 10. Depth profile of a 1.0 mm thick gel with $\mu_a = 10\ cm^{-1}$. The positive spike at 3.2 microseconds is from the black substrate on which the gel rested.

as deep as 800–900 μm. In Viator et al. [3], signals from layered turbid phantoms were detected as deep as 8 mm, which is an order of magnitude deeper than most PWS, indicating that the photoacoustic method is not depth limited for this intended clinical application. Combined with the depth profiling scheme described above, the photoacoustic method may provide a robust, non-invasive means for probing PWS anatomy.

CONCLUSION

The photoacoustic probe has determined PWS depth in human skin up to 570 μm. The high SNR indicates that it can be used to probe human skin deeper than a millimeter, which is sufficient for most PWS. Once this depth is known at a specific location on the lesion, CSC may be adjusted to optimize surface cooling while maximizing PWS treatment. For instance, if the epidermal-to-PWS distance is 350 μm, the clinician would adjust the CSC spurt duration to allow maximum epidermal cooling, without affecting the targeted PWS blood vessel temperature. Once the laser pulse is delivered, the increased temperature in the PWS would be high enough to cause irreversible damage, while the cooled epidermis would not reach damage threshold. The probe could be used at all treatment sites so that CSC parameters may be optimized on an individual patient basis, enabling more effective PWS treatment.

ACKNOWLEDGMENTS

We acknowledge the insightful advice of Z. Wang and G. Aguilar on the design of the photoacoustic probe and the help of Woody McCauley in the clinical experiments.

REFERENCES

1. Esenaliev RO, Karabutov AA, Oraevsky AA. Sensitivity of laser opto-acoustic imaging in detection of small deeply embedded tumors. J Select Topics Quantum Electron 1999; 5:981–988.
2. Viator JA, Jacques SL, Prahl SA. Depth profiling of absorbing soft materials using photoacoustic methods. J Select Topics Quantum Electron 1999;5:989–996.
3. Viator JA, Paltauf G, Jacques SL, Prahl SA. Design and testing of an endoscopic photoacoustic probe for determining treatment depth after photodynamic therapy of esophageal cancer. Proc SPIE 2001;4256.
4. van Gemert MJC, Nelson JS, Milner TE, Smithies DJ, Verkruysse W, de Boer JF, Lucassen GW, Goodman DM, Tanenbaum BS, Norvang LT, Svaasand LO. Non-invasive determination of port wine stain anatomy and physiology for optimal laser treatment strategies. Phys Med Biol 1997; 42:937–950.
5. Dover JS, Arndt KA. New approaches to the treatment of vascular lesions. Lasers Surg Med 2000;26:158–163.
6. Verkruysse W, Majaron B, Tanenbaum BS, Nelson JS. Optimal cryogen spray cooling parameters for pulsed laser treatment of port wine stains. Lasers Surg Med 2000;27:165–170.
7. Duck FA. Physical Properties of Tissue. A Comprehensive Reference Book. London: Academic Press; 1990.
8. Zhao Y, Chen Z, Saxer C, Xiang S, de Boer JF, Nelson JS. Phase-resolved optical coherence tomography and optical Doppler tomography for imaging blood flow in human skin with fast scanning speed and high velocity sensitivity. Optics Lett 2000;25:114–116.
9. Chen Z, Zhao Y, Srinivas SM, Nelson JS, Prakash N, Frostig RD. Optical Doppler tomography. J Select Topics Quantum Electron 1999;5:1134–1142.
10. Sathyam US, Prahl SA. Limitations in measurement of subsurface temperatures using pulsed photothermal radiometry. J Biomed Optics 1996;2:251–261.
11. Oraevsky AA, Jacques SL, Tittel FK. Determination of tissue optical properties by piezoelectric detection of laser-induced stress waves. Proc SPIE 1993;1882:86–101.
12. Paltauf G, Schmidt-Kloiber H, Guss H. Light distribution measurements in absorbing materials by optical detection of laser-induced stress waves. Appl Phys Lett 1996;69:1526–1528.
13. Fitzpatrick TB. The validity and practicality of sun-reactive skin types I through VI. Arch Dermatol 1998;124:869–871.
14. Jacques SL, McAuliffe DJ. The melanosome: Threshold temperature for explosive vaporization and internal absorption coefficient during pulsed laser irradiation. Photobiol 1991;53:769–775.
15. Vogel A, Nahen K, Theisen D, Noack J. Plasma formation in water by picosecond and nanosecond Nd:YAG laser pulses—Part I: Optical breakdown at threshold and superthreshold irradiance. IEEE J Select Topics Quantum Electron 1996; 3:847–860.
16. van Gemert MJC, Welch AJ, Pickering JW, Tan OT. Optical-Thermal Response of Laser-Irradiated Tissue. In: New York: Plenum Press; 1995.
17. Barsky SH, Rosen S, Greer DE, Noe JM. The nature and evolution of port wine stains: A computer-assisted study. J Invest Derm 1980;74:154–157.
18. Niechajev IA, Clodius L. Histology of port-wine stain. Eur J Plast Surg 1990;13:79–85.